

RESEARCH ARTICLE

10.1002/2016WR019047

Fate and transport of dissolved methane and ethane in cretaceous shales of the Williston Basin, Canada

M. Jim Hendry¹, S. Lee Barbour², Erin E. Schmeling¹, Scott O. C. Mundle³, and M. Huang²

Key Points:

- Correlations between dissolved Cl and CH₄ and C₂H₆ in Cretaceous shale suggest a lack of production or consumption of CH₄ and C₂H₆
- Depth profiles of Cl, CH₄, and C₂H₆ in the shale and 1-D solute transport modelling suggest long-term upward diffusion from deeper sources
- δ¹³C-CH₄ profiles in the shale are consistent with upward diffusional fractionation of isotopes from greater depths in the shale

Supporting Information:

- Supporting Information S1

Correspondence to:

M. J. Hendry,
jim.hendry@usask.ca

Citation:

Jim Hendry, M., S. Lee Barbour, E. E. Schmeling, S. O. C. Mundle, and M. Huang (2016), Fate and transport of dissolved methane and ethane in cretaceous shales of the Williston Basin, Canada, *Water Resour. Res.*, 52, doi:10.1002/2016WR019047.

Received 15 APR 2016

Accepted 28 JUL 2016

Accepted article online 8 JUL 2016

¹Department of Geological Sciences, University of Saskatchewan, Saskatoon, Saskatchewan, Canada, ²Department of Civil and Geological Engineering, University of Saskatchewan, Saskatoon, Saskatchewan, Canada, ³Great Lakes Institute for Environmental Research, University of Windsor, Windsor, Ontario, Canada

Abstract Baseline characteristics of dissolved methane (CH₄) and ethane (C₂H₆) and their stable isotopes in thick, low hydraulic conductivity, Cretaceous shales were determined using high-resolution core profiling at four sites in the Williston Basin (WB), Canada. Positive correlations with the conservative natural tracer Cl⁻ reflected a lack of measureable production or consumption of gases in the shale to the depth investigated (150 m below ground, BG) and suggest CH₄ and C₂H₆ concentrations near the interface with overlying Quaternary sediments are controlled by lateral migration and dilution in permeable zones. Curvilinear increasing concentrations with depth in the shale at all sites coupled with 1-D solute transport modeling suggest long-term (over millions of years) upward diffusion of CH₄ and C₂H₆ from deeper WB sources, likely the Second White Speckled Shale Formation (SWSS; ~790 m BG). δ¹³C-CH₄ profiles in the shale are consistent with upward diffusional fractionation of isotopes from the SWSS. Distinct CH₄ and C₂H₆ isotope values of gases in the shales versus ¹³C-enriched thermogenic isotopic signatures of CH₄ and C₂H₆ in deeper oil-producing WB intervals could be used to identify fugitive gases originating deeper in the Basin.

1. Introduction

Unconventional natural gas extraction from low hydraulic conductivity (*K*) sandstones, shales, and some coal beds is an important energy resource to meet growing global demand [U.S. Energy Information Administration, 2013]. However, development of these unconventional sources, as well as extraction of conventional oil/gas, carbon capture, and geological storage, have the potential to leak fugitive natural gases and fluids (most commonly via faulty annular well seals placed around the casing to prevent leakage of gas from a production well) into adjacent potable groundwater resources [Jackson *et al.*, 2013; Kargbo *et al.*, 2010; Osborn *et al.*, 2011]. These natural gases are typically dominated by methane (CH₄) but can include other low molecular weight, volatile hydrocarbons such as ethane (C₂H₆), propane, butane, and pentane. Few published peer-reviewed studies have been conducted on the effects of conventional and unconventional gas and oil (and carbon capture and geological storage) activities on potable groundwater resources to allow groundwater contamination issues to be addressed [Darrah *et al.*, 2014; Jackson *et al.*, 2013, and references therein].

Jackson *et al.* [2013] and Vidic *et al.* [2013] identify the need for baseline characterization of spatial and vertical variability in gas concentrations and their isotopic values to define future environmental concerns. Gas migration issues can result from poor well integrity [Darrah *et al.*, 2014; Szatkowski *et al.*, 2002] and geological seepage, both of which can be exacerbated by subsurface gas storage processes [Buzek, 1992; Goth, 1985]. Limited baseline gas data have been collected in shallow aquifers [cf., Aravena and Wassenaar, 1993; Darrah *et al.*, 2014; Harrison, 1983; McIntosh *et al.*, 2014]. Although Simpkins and Parkins [1993], Prinzhofner *et al.* [2009], and Clark *et al.* [2015] provide insights into the source of CH₄ in a glacial till, sources of isotopically light CH₄ in diffusion-dominated systems and origin and timing of methane generation in aquicludes, respectively, we are aware of no studies that characterize the distribution, origin, and fate of natural gases in low *K* argillaceous sediments. An understanding of CH₄ gas migration in argillaceous sediments is also required when considering these sediments as host rock formations for the disposal of high-level and long-lived radioactive waste because microbial degradation of organics proximal to the waste can result in the production of CH₄. If the rate of CH₄ production exceeds migration, free gases may form and, as gas pressures increase, free gas ingress could cause secondary pathways in the shale [Jacops *et al.*, 2013].

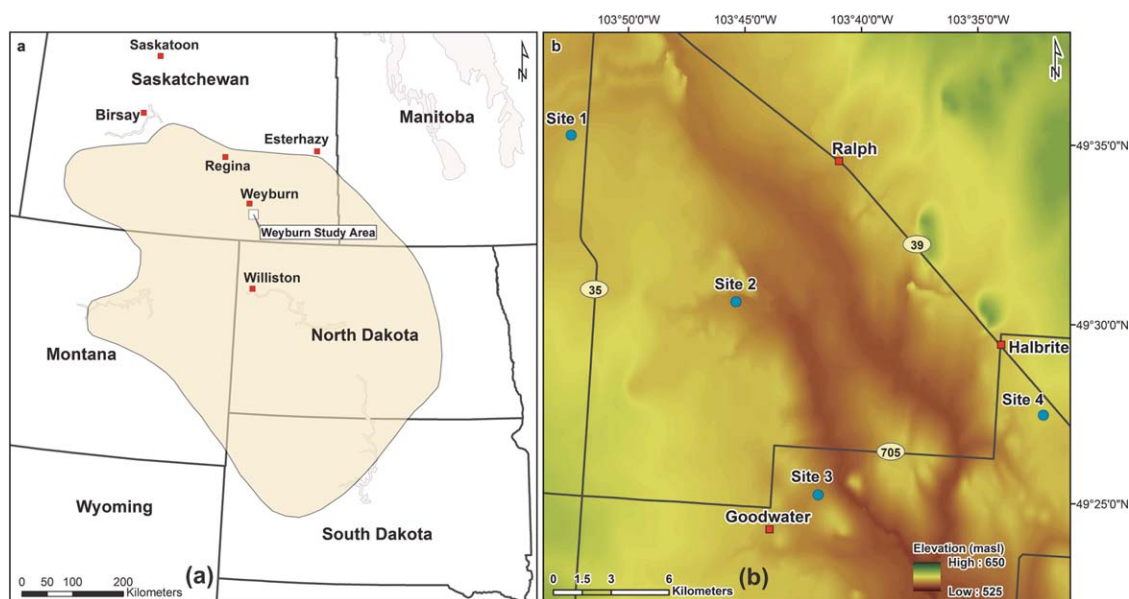


Figure 1. Location of the Weyburn study area within the Williston Basin (left) and topography, location of drill sites (solid blue circles), and towns (solid red squares) within the study area (right).

The current study was undertaken to improve upon the limited understanding of dissolved natural gases in argillaceous sediments. Generating porewater profiles through low K argillaceous sediments using conventional groundwater wells is, however, problematic. First, slow groundwater recharge rates will prohibit purging the standing water from these wells and result in mixed samples of altered and unaltered formation porewater [Wassenaar and Hendry, 1999]. This is especially true for volatile and reactive components of hydrocarbon gases. Second, the installation of enough wells to produce depth profiles of solutes through these sediments, that are often located at depth, can be cost prohibitive. Many of these limitations can be overcome by profiling the compositional and isotope values of CH_4 and the light alkanes from core samples collected during drilling programs. Recently, analyses of low-molecular weight hydrocarbon concentrations in the headspace of core samples stored in IsoJars® have been used to determine the concentrations of dissolved gases and values of associated isotopes [Clark *et al.*, 2015; Hendry *et al.*, 2016].

The objectives of this study were to: (1) characterize the distribution of naturally occurring conservative dissolved chloride (Cl^-) as well as CH_4 and C_2H_6 and their stable isotopes ($\delta^2\text{H}$ and $\delta^{13}\text{C}$) with depth through shale using core samples and; (2) identify the origin, mode of transport, and fate of these solutes. The objectives of the study were attained by interpreting four detailed depth profiles of dissolved Cl^- , CH_4 , and C_2H_6 and their stable isotopes from core samples collected at four sites located across a 200 km² area near Enhanced Oil Recovery (EOR) operations in the Williston Basin (WB) (Figure 1). Although this study was conducted across a relatively small area of the WB, similarities between the hydrogeology and solute transport (including CH_4) at these sites and other sites in Cretaceous shales across the Basin [Hendry and Harrington, 2014; Hendry *et al.*, 2011, 2013; Schmeling, 2014] suggest that our findings may be generally applicable to define baseline gas conditions that can be used to identify fugitive/stray gas migration from hydraulic fracturing and/or well integrity issues across the WB. The similarity between the solute transport in the Cretaceous shales in the WB and other low K argillaceous formations [Hendry *et al.*, 2015; Mazurek *et al.*, 2011] further suggests that these findings may be generally applicable to other shales. This study also provides additional detail to characterize the origin, fate, and transport of dissolved gases in fine-grained, low K argillaceous formations (e.g., clay-rich glacial till, shales).

2. Materials and Methods

Geological logging and continuous core sampling were conducted in stages at the four sites (Figure 1). Initially, drilling and coring were conducted at Site 1 to 100 m below ground (BG) in October 2012. Drilling and coring were subsequently conducted to 150 m BG at Site 2 and to 100 m BG at Sites 3 and 4 in

September 2013. Additional shallow drilling and coring (20 m BG) were conducted at Sites 2 and 4 in November 2013. All deep (≥ 100 m) drilling was performed using an Ingersoll Rand TH60 rotary drill rig and shallow drilling using a track mounted Diedrich d-120 hollow stem auger drill.

Continuous cores were collected during rotary drilling using continuous wireline coring methods and a solid core barrel with PVC liner (75 mm dia. \times 3.05 m long). Core samples (~ 10 –15 cm long) were collected at 1–10 m intervals. The outer 2–5 mm of all core samples were immediately removed after core retrieval to minimize contamination by drill mud. Core contamination by drill fluid was assessed by spiking the rotary drill water with 99% D₂O prior to and during drilling (details are presented in supporting information). Samples collected for squeezing and aqueous extract analyses were immediately placed in medium-sized (1100 mL) Ziploc™ polyethylene resealable bags with the atmospheric air squeezed out prior to sealing. Each bagged sample was subsequently placed in a large-sized (4600 mL) Ziploc™ polyethylene resealable bag and the atmospheric air again squeezed out prior to sealing. Trimmed core samples for gas analysis (CH₄, C₂H₆, O₂, and N₂) were immediately placed in Isojars® (~ 660 cm³), flushed with N₂ gas for 20 s, and sealed. All samples were placed in coolers at ambient temperature (20–25°C) and transported to the University of Saskatchewan (UofS) where they remained in coolers at room temperature until analysis.

Continuous coring during auger drilling was conducted using a split spoon core barrel and plastic liner (76 mm dia. \times 3.05 m long) at Sites 2 and 3. Site 4 was cored without the use of a liner (38 mm dia. \times 0.6 m long). Collection, handling, shipping, and analyses of the core samples were conducted as described for the continuous core drilling program above. Samples were collected in medium-sized Ziploc™ bags (1100 mL) for squeezing and samples for gas analyses were collected in Isojars® flushed with N₂ gas and sealed.

Porewater for Cl⁻ analyses was squeezed from core samples collected at 10 m intervals at Sites 1–4 during continuous core drilling and every 3 m for auger drilling coring. The core samples collected for squeezing were chipped, immediately packed into the squeeze cylinder (316 L stainless steel; 50 mm dia. \times 80 mm long), and subjected to high-pressure mechanical squeezing. The squeezer consisted of a piston inserted into the cylinder and loaded by a hydraulic press at 50 MPa. The operation and sampling protocol for the squeezing is described elsewhere [Hendry *et al.*, 2013]. Squeezed porewater samples were analyzed for Cl⁻ using a Dionex ICS-2100 ion chromatography system with an accuracy and precision of $\pm 5\%$ and a method detection limit of 0.5 mg/L.

Core samples collected at 1 m intervals during continuous core drilling at Site 1 were subjected to aqueous extraction (water-solid ratio of 3:1) for Cl⁻ analysis [Price, 2009]. The Cl⁻ concentrations of the aqueous water samples were analyzed using the method described above. These aqueous extract results were used to estimate the effective porosity (n_e) for Cl⁻ [Pearson, 1999; Waber and Smellie, 2008] by adjusting n_e until the extracted Cl⁻ concentrations were the same as the associated squeezed porewater Cl⁻ concentrations [Van Loon *et al.*, 2007] (method details are presented in supporting information). A direct comparison of corrected extracted Cl⁻ concentrations and corresponding squeezed porewater concentrations yielded a good fit ($y = 1.04x - 41.3$, $R^2 = 1.0$; $n = 9$; data not presented), showing that the corrected extracted concentrations reflect porewater concentrations.

Core samples placed in Isojars® were collected at 3 m intervals during continuous core drilling and 1 m intervals during auger drilling. The samples were allowed to equilibrate with the headspace in the Isojars® at standard temperature (25°C) and pressure (1 atm) for 31 and 101 days prior to analyses, respectively, at which time the gas headspace was analyzed for CH₄ and C₂H₆. About 10 cm³ of the gas headspace were collected from each IsoJar® in a 60 cm³ syringe and injected into the septa port of an Agilent 7890 gas chromatograph (GC) equipped with a flame ionization detector (FID) to measure light hydrocarbons and a thermal conductivity detector to measure O₂ and N₂. Based on analyses conducted on Scotty™ 17 L calibration gas standards (concentrations of 0.0010, 0.01, 0.1, and 10% CH₄ and 0.0010, 0.01, 0.1, and 1.0% C₂H₆) and on replicate core samples, the accuracy of the analytical method was $\pm 5\%$. The limit of detection (LOD) and limit of quantification (LOQ) for both CH₄ and C₂H₆ were determined to be 1.1 and 11 ppm, respectively.

Additional testing of IsoJar® samples collected from the shale at 82.4, 128.5, and 151.5 m BG during continuous core drilling at Site 2 was conducted to determine if the CH₄ and C₂H₆ concentrations measured in the Isojars® represent all available CH₄ and C₂H₆ gas in the samples (or also present in a solids-associated phase). These samples were analyzed for CH₄ and C₂H₆ after equilibrating for a 146 day period, after which the samples were flushed with N₂ gas for 20 s and resealed (termed the second flush). CH₄ concentrations

were analyzed after 1, 2, 5, 10, and 20 days (the end of the second flush test was determined based on the time required for the CH₄ concentration in the IsoJar® headspace to attain near steady state). After 20 days, the IsoJars® were again flushed with N₂ gas for 20 s and resealed (termed third flush) and CH₄ concentrations analyzed after another 1, 2, 5, 10, and 20 days. Concentrations of CH₄ measured in the headspace of the IsoJars® (ppmV) containing the core samples were converted to dissolved concentrations (mg/L) using the method outlined in *Kampbell and Vandegrift* [1998] and *Hendry et al.* [2016].

Measurement of $\delta^{13}\text{C}$ and $\delta^2\text{H}$ of CH₄ and $\delta^{13}\text{C}$ values of C₂H₆ samples collected in IsoJars® from the shale at Site 1 were measured at the University of Ottawa using an HP7890A GC interfaced to a Delta V Thermo isotope ratio mass spectrometer (IRMS). Accuracy and precision of this method were both estimated to be $\pm 0.3\text{‰}$. Measurement of CH₄ samples collected in IsoJars® from the shale at Sites 2–4 were performed at Isotope Tracer Technologies Inc. (Waterloo, Canada) on a Delta^{Plus}XL Thermo Finnigan IRMS coupled with an Agilent 6890 GC and a combustion or pyrolysis system. Accuracy and precision were better than $\pm 0.5\text{‰}$ [*Sherwood Lollar et al.*, 2007]. All $\delta^{13}\text{C}$ and $\delta^2\text{H}$ analyses were reported in permil (‰). For $\delta^{13}\text{C}$, the measurements are presented as relative to Vienna Pee Dee Belemnite (VPDB) and for $\delta^2\text{H}$ to Vienna Standard Mean Ocean Water (VSMOW). The detection limits of $\delta^{13}\text{C}$ and $\delta^2\text{H}$ were 0.05 and 0.20 mg/L, respectively.

3. Results and Discussion

3.1. Geology

The geology at each site consists of a complex series of Quaternary (till) deposits (36–77 m thick) overlying thick Cretaceous shale (supporting information Figure S1). The Quaternary deposits consist of the Saskatoon Group and the Sutherland Group glacial sediments. The Saskatoon Group is divided into the Battleford and Floral Formations and the Sutherland Group into the Warman, Dundurn, and Mennon Formations [*Christiansen*, 1992]. Stratified deposits (permeable zones) were encountered in the tills at Sites 1, 2, and 4. The Quaternary and Cretaceous sediments are separated by thin Paleocene-aged Ravenscrag Formation and Maastrichtian-aged Frenchman-Whitemud-Eastend Formation at Site 3. The Ravenscrag Formation consists of unconsolidated to poorly consolidated sands, silts, and clays. The Frenchman-Whitemud-Eastend Formation consists of coarse to fine-grained, cross-bedded sands interbedded with clays. The Pierre Shale Formation consists of noncalcareous, grey to dark grey, hard, high plasticity silt and clay [*Bilodeau and Potter*, 2012]. It is ~700 m thick at the EOR. The depositional ages of the geologic units encountered in the study area are presented in supporting information Table S1.

3.2. Chloride Profiles

Core contamination by drill fluids was limited, as indicated by comparison of the $\delta^2\text{H}$ of H₂O values measured on core samples to the $\delta^2\text{H}$ values of D₂O spiked drill fluids (see supporting information Figure S2). Data from core samples determined to be contaminated by drill fluids were not considered further.

Depth profiles of conservative dissolved Cl[−] are presented in Figure 2a. The deepest profile (Site 2) exhibits a curvilinear (concave down) depth trend in the Pierre Shale, starting at 1230 mg/L at the till-shale interface and increasing to 4240 mg/L at 135.8 m below the top of the Pierre Shale (TOS). The other shallower profiles are consistent with the upper part of the shale profile at Site 2. At all sites, there is a distinct break in slope (from curvilinear in the shale to near vertical in the till) at the TOS. The Cl[−] concentrations in the Quaternary sediments above this break range from 55 to 306 mg/L. The location of the upper Cl[−] boundary at the TOS is attributed to lateral flushing and dilution of Cl[−] at this depth and corresponds to the presence of permeable layers that can transmit solutes laterally within the Quaternary tills (Sites 1 and 2) or the Ravenscrag and Frenchman Formations (Site 3) (supporting information Figure S1). Although no permeable layer was observed at the upper boundary at Site 4, a permeable layer may be proximal to the borehole and, as such, control the solute profiles via diffusion. *Hendry and Wassenaar* [2009] and *Hendry et al.* [2000] document similar effects in a low *K* glacial till.

The curvilinear trend of increasing concentration with depth in the shale is consistent with a conceptual model in which initially linear Cl[−] profiles develop across the shale as a result of long-term upward diffusion from greater depths. The subsequent perturbation of the upper concentration boundary near the TOS by glaciation led to the establishment of a new upper concentration boundary at the TOS, reflected in the curvature in the profile. This conceptual model is based on the dominant transport mechanism in the shales

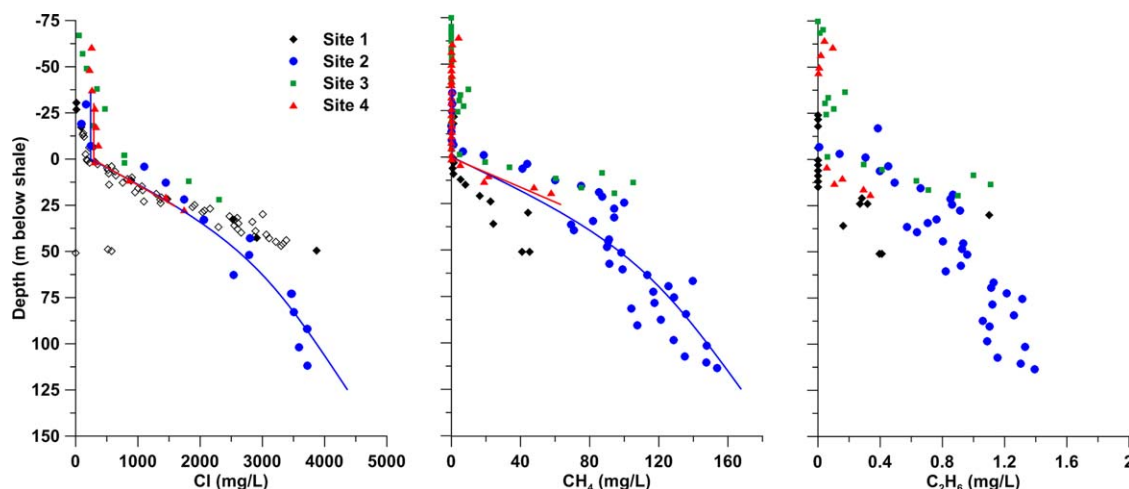


Figure 2. Dissolved (a) Cl^- , (b) CH_4 , and (c) C_2H_6 concentrations versus depth below top of Pierre Shale at drill sites. The solid and open (Site 1) symbols in (a) are analyses on squeezed pore waters and pore water concentrations calculated from aqueous extract analyses, respectively. Simulated profiles for Site 2 (blue line) and Site 4 (red line) for Cl^- and CH_4 are presented (see supporting information section 4.1). The simulated times represent total diffusion times of 1.4 and 1.2 Ma for Cl^- and CH_4 since the deposition of the tills on top of evolved pre-Quaternary profiles at Site 4 and a time of 1.2 Ma for both Cl^- and CH_4 since the deposition of the tills on top of evolved pre-Quaternary profiles at Site 2.

being diffusion. This assumption is supported by the low measured K values (10^{-12} – 10^{-13} m/s) [Smith *et al.*, 2016] and advection-diffusion transport modeling [Hendry *et al.*, 2013] in the Pierre Shale, the curvilinear shape of the concentration profiles being consistent with diffusive transport and not advective transport, and solute transport studies in several other argillaceous systems [cf., Desaulniers *et al.*, 1986; Gimmi *et al.*, 2007; Hendry and Harrington, 2014; Hendry *et al.*, 2000, 2011, 2015; Mazurek *et al.*, 2011; Patriarche *et al.*, 2004; Rubel *et al.*, 2002]. In the current study, the source of the Cl^- is below the base of exploration (>200 m BG). Based on analyses of mine inflow samples collected vertically through the WB, Hendry and Harrington [2014] conclude that the source of the Cl^- in the Cretaceous shales could be long-term upward diffusion from the Prairie Evaporite, located about 1440 m BG in the current study area [White *et al.*, 2004]. A similar near linear increase in Cl^- concentration with depth to that observed across the study area was measured through 275 m of Lower Cretaceous argillaceous sediments in the WB by Hendry and Harrington [2014]. Based on the shape of the profile and 1-D transport modeling, they attributed the linear depth trend to long-term (over a 20–25 Ma period) upward diffusion from deeper basinal sediments. A near-linear Cl^- -depth profile through 130 m of the Boom Clay at Essen, Belgium was also attributed to long-term (>1.4 Ma) steady state diffusion [Mazurek *et al.*, 2011].

3.3. Dissolved Methane and Ethane Concentrations

CH_4 and C_2H_6 concentrations were determined from gas measurements on the headspaces of the IsoJars[®] samples. The degree of atmospheric leakage into the IsoJars[®], and thus contamination of the headspace samples during sampling and storage, was determined by measuring the O_2 concentrations in the headspaces of core samples (jars were flushed with N_2). Based on these data (not presented), only analytical data from IsoJars[®] with <2.0 mol. % O_2 were determined to approximate in situ concentrations (i.e., no O_2 should exist in anoxic core sediments containing CH_4 ; thus, the presence of O_2 in IsoJars[®] can only be attributed to the ingress of O_2 into the IsoJars[®] and, as a result, a concomitant loss of core CH_4 and C_2H_6 from the IsoJars[®]). This cutoff is consistent with the observation that CH_4 concentrations measured in most of the high O_2 IsoJars[®] show at least a 50% reduction when compared to measurements from samples taken above or below (± 3 m). The ingress of O_2 and loss of CH_4 and C_2H_6 in these IsoJars[®] is attributed to poor seals. Using this cutoff for O_2 concentrations, about 15% of the IsoJars[®] were considered contaminated and their gas analyses data were not considered further.

The CH_4 and C_2H_6 concentrations in the headspace of the IsoJar[®] samples from core samples collected from the shale and glacial sediments at Site 1 and after equilibration times of 31 and 101 days (supporting information Figure S3) show strong linear correlations between the data sets; the R^2 of the CH_4 and C_2H_6 concentrations were 0.96 and 0.36 in the glacial till and 0.93 and 0.81 in the shale, respectively. Both shale

data sets yielded slopes near 1 (1.0 and 0.9, respectively). These observations demonstrate that CH₄ and C₂H₆ concentrations in the IsoJar[®] shale samples attained equilibrium within 31 days and that no measurable loss of CH₄ or C₂H₆ to oxidation was detected during core storage. Because each jar is expected to contain a finite concentration of gases and leaking/oxidation will affect each gas sample differently, the constant composition of the headspace gases in the jars over a 16 month test period (within analytical uncertainty; data not shown) provides strong supporting evidence that equilibrium was attained. The attainment of equilibrium gas concentrations in shale cores placed in the IsoJar[®] by 31 days was supported by multiphase diffusion modeling of CH₄ [Hendry *et al.*, 2016] from core. Hendry *et al.* [2016] also show till and shale core samples from the current study area treated with and without an antimicrobial agent exhibit no measurable effects on the CH₄ and C₂H₆ concentrations from the core samples over storage times used in the current study, consistent with a lack of oxidation during storage in the jars.

The potential for release of CH₄ and C₂H₆ from the solids to the gas fraction in the IsoJars[®] samples was tested by measuring headspace CH₄ and C₂H₆ concentrations in IsoJars[®] containing shale core samples from 82.4, 128.5, and 151.5 m BG at Site 2 after sequential flushing with inert gas (supporting information Figure S4). The CH₄ concentrations (supporting information Figure S4a) increased from 0 ppmV after the first flush of N₂ on day 0 to 32,610–53,010 ppmV after 31 days. No changes in concentrations were measured between day 101 and 146, suggesting equilibrium concentrations were attained. After the IsoJars[®] were flushed with N₂ on day 146 (flush 2), CH₄ concentrations increased from 0 to 367–514 ppmV on day 10, after which the concentrations did not change. Twenty days after the second flush, the concentrations were consistent with those measured after 10 days. After the IsoJars[®] were flushed with N₂ gas on day 172 (flush 3), CH₄ concentrations increased from 0 to 50–77 ppmV after 20 days. These tests show that, over the time period tested, >99% of the readily releasable CH₄ in the core was released into the headspace of the IsoJars[®] during the first flush and suggest that this CH₄ is accessible to the porewater. Chalmers and Bustin [2008] conclude that the CH₄ sorption capacity in Lower Cretaceous shale samples increases with increasing total organic carbon (TOC) content. Their data show a lack of sorption capacity for TOC concentrations <2 wt. %. The low TOC values in the shales (mean = 0.86 ± 0.4; n = 35; supporting information Table S2) suggest a lack of CH₄ sorption capacity in the shales and imply that the measured porewater-accessible CH₄ represents the CH₄ in the cores. Results of the time series analyses during the second N₂ gas flush (supporting information Figure S4a) indicate that the CH₄ in the shale attains equilibrium with the headspace in the IsoJars[®] in <10 days, which aligns with equilibration times in supporting information Figure S3 (i.e., <31 days) and is consistent with an estimate of 4 days for fine-textured samples from the Michigan Basin also based on IsoJars[®] measurements [Clark *et al.*, 2015].

Consistent with the CH₄ concentrations in the sequential flushing experiments, C₂H₆ concentrations (supporting information Figure S4b) increased from 0 ppmV after the first flush of N₂ on day 0 to 152–509 ppmV after 31 days. No change in concentrations was measured between day 101 and 146, suggesting equilibrium concentrations had been reached. During the second and third flush, C₂H₆ concentrations were below the method quantification limit. These data suggest that the majority of the readily releasable C₂H₆ is released from the core during the first flush and that most of this C₂H₆ in the cores is also readily accessible to the porewater.

3.4. Dissolved Methane and Ethane Depth Profiles

Depth profiles were plotted for dissolved CH₄ (Figure 2b and supporting information Figure S5) and C₂H₆ (Figure 2c) measured in the IsoJars[®] after a 101 day equilibration period. CH₄ concentrations are low and constant with depth through the glacial sediments, ranging from 0.89 to 1.35 mg/L. CH₄ concentrations then exhibit an increase with depth through the Pierre Shale, attaining a concentration of about 150 mg/L at 120 m below the TOS (Site 2). CH₄ concentrations in the Ravenscrag and Frenchman Formation sediments at Site 3 were low, ranging from 0.03 to 6.75 mg/L. Although the CH₄ concentrations in the thicker shale sequences (i.e., Site 2) reflect a slightly concave increase with depth, the concentrations are variable (±25 mg/L). This variability inversely corresponds to O₂ concentrations of 0.3–1.2 mol. % measured in the shale IsoJars[®] from Site 2 (data not presented). The greater O₂ concentrations are associated with the lower CH₄ concentrations and suggest the lower CH₄ concentrations may be analytical artifacts from the introduction of atmospheric gas into and dissolved gases from the jars. Thus, the maximum values in the concentration-depth CH₄ profiles may best represent the in situ profiles.

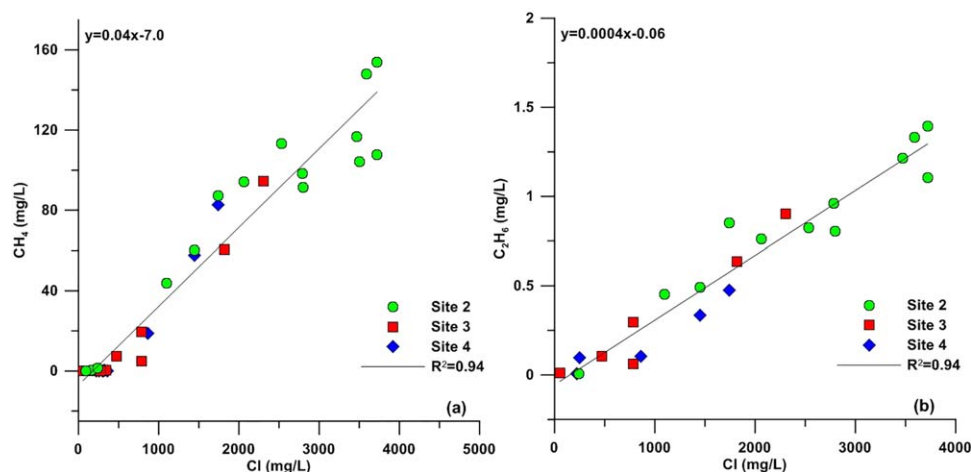


Figure 3. Measured Cl^- versus calculated (a) CH_4 and (b) C_2H_6 concentrations based on headspace gas measurements.

Consistent with observations for CH_4 , concentrations of C_2H_6 increase with depth. Low concentrations of C_2H_6 (often below the detection limit) are observed with depth through the glacial sediments (0.01–0.39 mg/L) and concentrations increase with depth through the Pierre Shale (maximum concentration of 1.4 mg/L at 120 m below the TOS; Site 2). Ravenscrag and Frenchman Formation sediments at Site 3 yielded low C_2H_6 concentrations (0.05–0.17 mg/L). The concave downward shape of the C_2H_6 profile in the thicker shale sequences (Site 2) is consistent with those for CH_4 and Cl^- .

The dissolved CH_4 and C_2H_6 concentration-depth profiles are positively correlated with the associated Cl^- profiles. The cross-plotted CH_4 versus Cl^- concentrations and C_2H_6 and Cl^- concentrations yield strong linear relationships ($R^2 = 0.94$ and 0.94 , respectively; Figure 3). The slightly curvilinear nature of the CH_4 and C_2H_6 depth-profiles in the shale for all sites suggests that the transport mechanism for these gases is similar to that for Cl^- (i.e., upward diffusion through the shale with the dominant source area being below the base of exploration). The strong correlations with conservative Cl^- also suggest a lack of biogeochemical activity in the CH_4 and C_2H_6 concentration-depth profiles (i.e., no production or consumption) in the shale.

The low CH_4 and C_2H_6 concentrations in the tills immediately above the shale at the study sites show removal of CH_4 and C_2H_6 over a short vertical distance (<3 m). The concomitant decreases in conservative Cl^- concentrations at similar depth intervals suggest the decrease in CH_4 and C_2H_6 concentrations are in large part the result of the same mechanism as for Cl^- —lateral migration in more permeable sediments, however, the removal of some CH_4 and C_2H_6 from the permeable zones or associated CH_4 oxidation cannot be ruled out.

As was the case for Cl^- , the curvilinear shape of the CH_4 and C_2H_6 depth profiles in the shale can be explained by long-term, near steady state diffusion from a source located below the base of exploration (>200 m BG), followed by a more recent perturbation of the TOS. The Second White Speckled Shale Formation (SWSS; located ~790 m BG in the study area) is a possible source for both gases. Hendry *et al.* [2011] identify the greatest CH_4 concentrations (ppmV) in Cretaceous shales at a site 160 km east of the current study area in the SWSS (at 256–321 m BG), with concentrations decreasing with distance above and below this unit. The nearly linear CH_4 -depth profiles in the shale are similar to CH_4 concentration profiles collected over a 5 m thickness of anoxic marine sediments by Barnes and Goldberg [1976], who also attribute the CH_4 depth trend to upward diffusion of CH_4 .

3.5. Transport and Timing of Chloride and Methane Migration

The transport, timing, and fluxes of Cl^- and CH_4 were modeled at Sites 2 and 4. The upper boundaries of Cl^- and CH_4 transport were at the TOS and reflected the point at which lateral migration of both Cl^- and CH_4 occurs. Details of the modeling approach (including initial and boundary conditions), transport parameters used, and results are presented in supporting information Figures S6, S7 and Table S3. An acceptable fit between 1-D modeling results and measured data show that diffusive transport without consideration of

microbial activity can adequately explain the measured CH_4 and the conservative Cl^- profiles. The presence of a diffusion-dominated transport system is consistent with the findings that biogeochemical activity could be a minor process in argillaceous aquitards [Lawrence *et al.*, 2000].

The time required to generate near steady state profiles in the shale at these sites could be very long—on the order of 100 Ma. Simulations of the evolution of the profile over a period of 72 Ma (time since shale deposition) were used to establish near steady state Cl^- profiles followed by various elapsed times for deposition of the Sutherland and Saskatoon Group tills. The best-fit simulated profiles for Cl^- and CH_4 at Sites 2 and 4 are presented in Figure 2. Although simulations reflect transport times of several tens of millions of years, the simulated profiles cannot be considered unique because of our lack of knowledge of the initial shale profiles (prior to glaciation), a poor understanding of the hydrogeologic history of the shale and tills, and the location of and concentrations in the source zones for both Cl^- and CH_4 .

3.6. Isotopes of Methane and Ethane

$\delta^{13}\text{C}$ and $\delta^2\text{H}$ values of CH_4 from the shale samples are plotted versus depth in Figure 4. The range of $\delta^2\text{H}-\text{CH}_4$ (-317 to -93‰), $\delta^{13}\text{C}-\text{CH}_4$ (-86 to -43‰), and $\delta^{13}\text{C}-\text{C}_2\text{H}_6$ (-60 to -52‰) values for shale samples are comparable to those measured in other shallow geologic environments, including groundwaters in Alberta and Saskatchewan [Cheung *et al.*, 2010; Taylor *et al.*, 2000], Ontario [McIntosh *et al.*, 2014], England [Darling and Goody, 2006], and Iowa [Simpkins and Parkins, 1993]. The $\delta^{13}\text{C}-\text{CH}_4$ values from the shale exhibit an overall ^{13}C -enrichment with increasing depth. The depth trend for the most extensive data set, at Site 2, yields a strong linear depth relationship from -86‰ at the TOS to -70‰ at 115 m below the TOS ($R^2 = 0.81$).

A linearly increasing trend with depth is also observed for $\delta^{13}\text{C}-\text{C}_2\text{H}_6$ at Site 2 from -56‰ at the TOS to -53‰ at 115 m below the TOS ($R^2 = 0.74$). A limited number of $\delta^{13}\text{C}-\text{C}_2\text{H}_6$ values were available from depths near the TOS for Sites 3 and 4. $\delta^{13}\text{C}-\text{C}_2\text{H}_6$ values were ^{13}C -depleted; however, several $\delta^{13}\text{C}-\text{CH}_4$ and $\delta^2\text{H}-\text{CH}_4$ were ^{13}C -enriched compared to Site 2 (Figure 4). The ^{13}C - and ^2H -enriched CH_4 values suggest microbial methane oxidation may have altered the isotope values of these samples; however, it is not known if this was attributable to poor seals on some of the sample jars, or if microbial activity may have also affected the $\delta^{13}\text{C}-\text{C}_2\text{H}_6$ in these samples. Unlike the $\delta^{13}\text{C}-\text{CH}_4$ and $-\text{C}_2\text{H}_6$ values, the $\delta^2\text{H}-\text{CH}_4$ values from shale samples exhibit no clear depth trend as evidenced by a poorer linear depth relationship for Site 2 data below the TOS ($R^2 = 0.33$); however, the $\delta^2\text{H}-\text{CH}_4$ values exhibit a more defined linear depth trend at depths >55 m below the TOS. Based on the linear trend of the isotopic values, the projected $\delta^{13}\text{C}-\text{CH}_4$ end-member at the base of exploration in the shales ($\delta^2\text{H}-\text{CH}_4 = -220\text{‰}$, and $\delta^{13}\text{C}-\text{CH}_4 = -70\text{‰}$) is consistent with values reported from the Colorado Group in the WB, where the most likely source zone in the area is the SWSS ($\delta^{13}\text{C}-\text{CH}_4 \sim -65\text{‰}$) [Rowe and Muehlenbachs, 1999; Szatkowski *et al.*, 2002; Tilley and Muehlenbachs, 2006]. Although greater variability is observed for $\delta^{13}\text{C}-\text{C}_2\text{H}_6$ values in the WB, the $\delta^{13}\text{C}-\text{C}_2\text{H}_6$ end-member at the base of exploration in the shales ($\delta^{13}\text{C}-\text{C}_2\text{H}_6 = -53\text{‰}$) is also consistent with isotope values reported for the SWSS ($\delta^{13}\text{C}-\text{C}_2\text{H}_6 \sim -50\text{‰}$) [Rowe and Muehlenbachs, 1999; Tilley and Muehlenbachs, 2006].

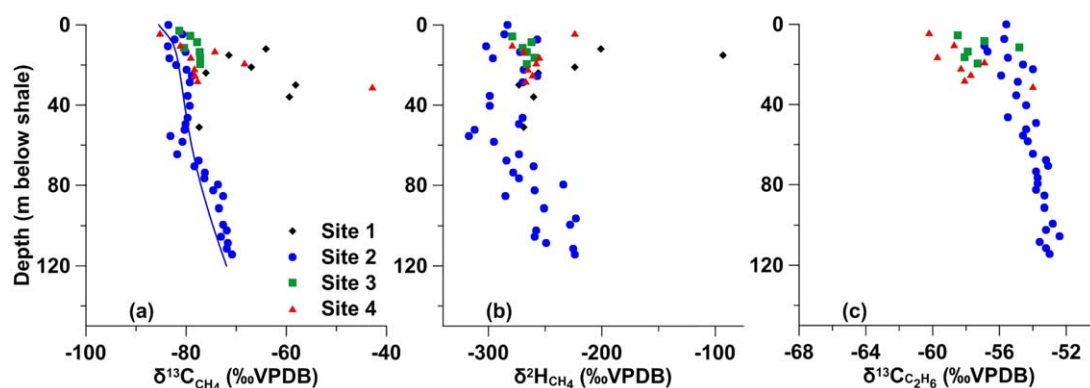


Figure 4. Depth profiles of (a) $\delta^{13}\text{C}$ and (b) $\delta^2\text{H}$ values of CH_4 and (c) $\delta^{13}\text{C}$ of C_2H_6 values from core samples versus depth below top of Pierre Shale at drill sites. The simulated $\delta^{13}\text{C}-\text{CH}_4$ profile for Site 2 (blue line) is presented in Figure 4a (see also supporting information section 4.2).

The literature provides no clear explanation for the large, well-defined changes in $\delta^{13}\text{C}\text{-CH}_4$ values ($>5\%$) with depth, such as those observed through the shale at Site 2 [Xia and Tang, 2012]. Some authors attribute the changes to the effects of CH_4 transport in the subsurface [Prinzhofer and Huc, 1995; Prinzhofer and Pernaut, 1997; Zhang and Krooss, 2001] while others invoke biological mechanisms and discount the effects of $\delta^{13}\text{C}\text{-CH}_4$ migration on $\delta^{13}\text{C}$ values [Fuex, 1980]. The different magnitude of isotopic fractionation between the CH_4 and C_2H_6 across the shale is consistent with diffusional fractionation, as the smaller difference in isotope mass ratio for C_2H_6 relative to CH_4 is expected to produce less diffusive isotopic fractionation. Transport modeling of the evolution of the $\delta^{13}\text{C}\text{-CH}_4$ depth profile through the shale at Site 2 (detailed in supporting information section 3.2) highlights that a profile similar to that observed (to a depth of approximately 120 m into the shale) can be obtained using similar transport conditions to those used for the CH_4 simulations. Results of this (nonunique) simulation highlight that present day $\delta^{13}\text{C}\text{-CH}_4$ profiles can be caused by diffusion fractionation in the shales. The similarity in the depth trends between $\delta^{13}\text{C}\text{-CH}_4$ and $\text{-C}_2\text{H}_6$ (Figure 4) could suggest the trend in $\delta^{13}\text{C}\text{-C}_2\text{H}_6$ also be attributed to diffusional fractionation, although further study would be required.

4. Conclusions and Implications

Characterizing the origin, distribution, and transport of dissolved natural gases and their isotopic signatures through low K argillaceous cap rock can be critical for assessing the source and pathways of stray gas contamination from, for example, hydraulic fracturing, CO_2 sequestration, or geological storage reservoirs. Leaking oil/gas wells pose an environmental and safety concern. They are a source of atmospheric CH_4 (climate change) and a potential explosion hazard [Baldassare and Laughrey, 1997]. This study presents, for the first time, a baseline characterization of the distribution, origin, and fate of CH_4 and C_2H_6 dissolved in groundwater in low K shale.

The strong linear correlations between the CH_4 , C_2H_6 , and conservative Cl^- concentrations in the shale suggest that CH_4 and C_2H_6 can be considered conservative species over the thickness of shale studied (115 m). The shape of the Cl^- , CH_4 , and C_2H_6 depth profiles and solute transport modeling of the CH_4 and Cl^- profiles indicate that they are the result of long-term (many millions of years) upward diffusion. The general shape of the Cl^- , CH_4 , and C_2H_6 profiles through the shales is consistent with Cl^- and CH_4 depth profiles in the upper Cretaceous shales at another site located 170 km NE [Hendry and Harrington, 2014; Hendry et al., 2011] of the study area. These similarities suggest that the profiles presented here and their interpretations may represent baseline conditions in the thick Cretaceous shales across the WB.

Stable isotope values of CH_4 from deeper oil-associated production zones in the Cretaceous (i.e., Mannville Formation), Jurassic, and Triassic of the WB are typically ^{13}C -enriched, reflecting a thermogenic origin [Cheung et al., 2010; Tilley and Muehlenbachs, 2006, 2007]. The differences in gas signatures between the deeper production zones and the Pierre Shale suggest that the isotopes of CH_4 and C_2H_6 may provide a means of identifying the presence of fugitive gases derived from deeper sources in the near surface environment. Mixing trends between the $\delta^{13}\text{C}\text{-CH}_4$ end-members at the study sites and conceptual modeling are consistent with long-term, diffusion-based transport of Cl^- and CH_4 .

Additional studies on the fate and transport of dissolved gases are warranted. These should include investigations into defining and interpreting: (1) depth trends of CH_4 and C_2H_6 in other argillaceous deposits, (2) depth trends of other low molecular weight, volatile hydrocarbons such as propane, butane, pentane, and their isotopes in shales, (3) depth trends of other redox sensitive dissolved species (e.g., sulfate) on organic gases, with a focus on the upper boundary condition, and (4) assessing the extent and importance of diffusional isotopic fractionation at the basin scale. These studies may provide additional information on the sources, transport mechanisms, and timing of evolution of CH_4 concentration with depth and the isotopes of CH_4 . Our findings also suggest additional study of the $\delta^{13}\text{C}\text{-CH}_4$ and $\text{-C}_2\text{H}_6$ profiles could provide insights to further refine the timing of the development and migration of CH_4 and C_2H_6 associated with the depositional histories of glacial tills and geochemical control(s) on CH_4 and C_2H_6 .

Acknowledgments

Support was provided by Cenovus Energy and funding from an NSERC-IRC (grant 184573) to M.J.H. Valuable hydrogeologic insights were provided by M. Dubord. All data used for producing figures and graphs in this manuscript are available in supporting information.

References

- Aravena, R., and L. I. Wassenaar (1993), Dissolved organic-carbon and methane in a regional confined aquifer, southern Ontario, Canada: Carbon-isotope evidence for associated subsurface sources, *Appl. Geochem.*, 8(5), 483–493.
- Baldassare, F. J., and C. D. Laughrey (1997), Identifying the sources of stray methane by using geochemical and isotopic fingerprinting, *Environ. Geosci.*, 4(2), 85–94.

- Barnes, R. O., and E. D. Goldberg (1976), Methane production and consumption in anoxic marine sediments, *Geology*, *4*, 297–300.
- Bilodeau, D., and G. Potter (2012), Weyburn core hole project: Coring, drilling and instrumentation, report SNC Lavalin.
- Buzek, F. (1992), Carbon isotope study of gas migration in underground gas-storage reservoirs, Czechoslovakia, *Appl. Geochem.*, *7*(5), 471–480.
- Chalmers, G. R. L., and R. M. Bustin (2008), Lower Cretaceous gas shales in northeastern British Columbia, Part I: Geological controls on methane sorption capacity, *Bull. Can. Petrol. Geol.*, *56*(1), 1–21.
- Cheung, K., P. Klassen, B. Mayer, F. Goodarzi, and R. Aravena (2010), Major ion and isotope geochemistry of fluids and gases from coalbed methane and shallow groundwater wells in Alberta, Canada, *Appl. Geochem.*, *25*(9), 1307–1329.
- Christiansen, E. A. (1992), Pleistocene stratigraphy of the Saskatoon Area, Saskatchewan, Canada: An update, *Can. J. Earth Sci.*, *29*, 1767–1778.
- Clark, I. D., D. Ilin, R. E. Jackson, M. Jensen, I. Kennell, H. Mohammadzadeh, A. Poulain, T. P. Zing, and K. G. Raven (2015), Paelozoic-aged microbial methane in an Ordovician shale and carbonate aquiclude of the Michigan Basin, southwestern Ontario, *Org. Geochem.*, *83–84*, 118–126.
- Darling, W. G., and D. C. Goody (2006), The hydrogeochemistry of methane: Evidence from English groundwaters, *Chem. Geol.*, *229*(4), 293–312.
- Darrah, T. H., A. Vengosh, R. B. Jackson, N. R. Warner, and R. J. Poreda (2014), Noble gases identify the mechanisms of fugitive gas contamination in drinking-water wells overlying the Marcellus and Barnett Shales, *Proc. Natl. Acad. Sci. U. S. A.*, *111*(39), 14,076–14,081.
- Desaulniers, D. E., J. A. Cherry, R. S. Kaufmann, and H. W. Bentley (1986), ^{37}Cl - ^{35}Cl variations in a diffusion controlled groundwater system, *Geochim. Cosmochim. Acta*, *50*, 1757–1764.
- Fuex, A. N. (1980), Experimental evidence against an appreciable isotopic fractionation of methane during migration, *Org. Geochem.*, *12*, 725–732.
- Gimmi, T., H. N. Waber, A. Gautschi, and A. Rübél (2007), Stable water isotopes in pore water of Jurassic argillaceous rocks as tracers for solute transport over large spatial and temporal scales, *Water Resour. Res.*, *43*, W04410, doi:10.1029/2005WR004774.
- Goth, M. (1985), Indication of methane movement from petroleum reservoir to surface, Loningén oilfield, northwest Germany, *J. Geochem. Explor.*, *23*(1), 81–97.
- Harrison, S. S. (1983), Evaluating system for ground-water contamination hazards due to gas-well drilling on the glaciated Appalachian plateau, *Ground Water*, *21*, 689–700.
- Hendry, M. J., and G. G. Harrington (2014), Comparing vertical profiles of natural tracers in the Williston Basin to estimate the onset of deep aquifer activation, *Water Resour. Res.*, *50*, 6496–6506, doi:10.1002/2014WR015652.
- Hendry, M. J., and L. I. Wassenaar (2009), Inferring heterogeneity in aquitards using high-resolution dD and d18O profile, *Ground Water*, *47*(5), 639–645.
- Hendry, M. J., L. I. Wassenaar, and T. Kotzer (2000), Chloride and chlorine isotopes (^{36}Cl and $\delta^{37}\text{Cl}$) as tracers of solute migration in a thick, clay-rich aquitard system, *Water Resour. Res.*, *36*(1), 285–296.
- Hendry, M. J., B. Richman, and L. I. Wassenaar (2011), Correcting for methane interferences on $\delta^2\text{H}$ and $\delta^{18}\text{O}$ measurements in pore water using $\text{H}_2\text{O}_{(\text{liquid})}$ - $\text{H}_2\text{O}_{(\text{vapour})}$ equilibration laser spectroscopy, *Anal. Chem.*, *83*(14), 5789–5796.
- Hendry, M. J., S. L. Barbour, K. Novakowski, and L. I. Wassenaar (2013), Palaeo-hydrogeology of the Cretaceous sediments of the Williston Basin using stable isotopes of water, *Water Resour. Res.*, *49*, 4580–4592, doi:10.1002/wrcr.20321.
- Hendry, M. J., D. K. Solomon, M. Person, L. I. Wassenaar, W. P. Gardner, I. D. Clark, K. U. Mayer, T. Kunimaru, K. Nakata, and T. Hasegawa (2015), Can argillaceous formations isolate nuclear waste? Insights from isotopic, noble gas, and geochemical profiles, *Geofluids*, *15*(3), 381–386, doi:10.1111/gfl.12132.
- Hendry, M. J., S. L. Barbour, E. Schmeling, and S. O. C. Mundle (2016), Measuring concentrations of dissolved methane and ethane and ^{13}C of methane in shale and till, *Ground Water*, doi:10.1111/gwat.12445, in press.
- Jackson, R. E., A. W. Gorody, B. Mayer, J. W. Roy, M. C. Ryan, and D. R. Van Stempvoort (2013), Groundwater protection and unconventional gas extraction: The critical need for field-based hydrogeological research, *Ground Water*, *51*(4), 488–510, doi:10.1111/gwat.12074.
- Jacops, E., G. Volckaert, N. Maes, E. Weetjens, and J. Govaerts (2013), Determination of gas diffusion coefficients in saturated porous media: He and CH_4 diffusion in Boom Clay, *Appl. Clay Sci.*, *83–84*, 217–223.
- Kampbell, D. H., and S. A. Vandegrift (1998), Analysis of dissolved methane, ethane, and ethylene in ground water by a standard gas chromatographic technique, *J. Chromatogr. Sci.*, *36*, 253–256.
- Kargbo, D. M., R. G. Wilhelm, and D. J. Campbell (2010), Natural gas plays in the Marcellus Shale: Challenges and potential opportunities, *Environ. Sci. Technol.*, *44*(15), 5679–5684.
- Lawrence, J. R., M. J. Hendry, L. I. Wassenaar, G. M. Wolfaardt, J. J. Germida, and C. W. Greer (2000), Distribution and biogeochemical importance of bacterial populations in a thick clay-rich aquitard system, *Microb. Ecol.*, *40*, 273–291.
- Mazurek, M., et al. (2011), Natural tracer profiles across argillaceous formations, *Appl. Geochem.*, *26*(7), 1035–1064, doi:10.1016/j.apgeochem.2011.03.124.
- McIntosh, J. C., S. E. Grasby, S. M. Hamilton, and S. G. Osborne (2014), Origin, distribution and hydrogeochemical controls on methane occurrences in shallow aquifers, southwestern Ontario, Canada, *Appl. Geochem.*, *50*, 37–52.
- Osborn, S., A. Vengosh, N. R. Warner, and R. B. Jackson (2011), Methane contamination of drinking water accompanying gas-well drilling and hydraulic fracturing, *Proc. Natl. Acad. Sci. U. S. A.*, *108*, 8172–8176.
- Patriarche, D., J. Michelot, E. Ledoux, and S. Savoye (2004), Diffusion as the main process for mass transport in very low water content argillites: 1. Chloride as a natural tracer for mass transport: Diffusion coefficient and concentration measurements in interstitial water, *Water Resour. Res.*, *40*, W01516, doi:10.1029/2003WR002600.
- Pearson, F. J. (1999), What is the porosity of a mudrock? In *Muds and Mudstones: Physical and Fluid Flow Properties*, *Geol. Soc. Spec. Publ.*, *158*, 9–21.
- Price, W. A. (2009), Prediction manual for drainage chemistry from sulphidic geologic materials, *MEND Rep. 1.20.1*. [Available at <http://mend-nedem.org/category/uncategorized/>]
- Prinzhofer, A. A., and A. Y. Huc (1995), Genetic and post-genetic molecular and isotopic fractionations in natural gases, *Chem. Geol.*, *126*(3–4), 281–290.
- Prinzhofer, A. A., and E. Pernaton (1997), Isotopically light methane in natural gas: Bacterial imprint or diffusive fractionation?, *Chem. Geol.*, *142*(3–4), 193–200.
- Prinzhofer, A., J. P. Girard, S. Buschaert, Y. Huiban, and S. Noirez (2009), Chemical and isotopic characterization of hydrocarbon gas traces in porewater of very low permeability rocks: The example of the Callovo-Oxfordian argillites of the eastern part of the Paris Basin, *Chem. Geol.*, *260*, 269–277.
- Rowe, D., and K. Muehlenbachs (1999), Isotopic fingerprints of shallow gases in the Western Canadian sedimentary basin: Tools for remediation of leaking heavy oil wells, *Org. Geochem.*, *30*(8A), 861–871.

- Rübel, A. R., C. Sonntag, J. Lippmann, F. J. Pearson, and A. Gautschi (2002), Solute transport in formations of very low permeability: Profiles of stable isotope and dissolved noble gas contents of pore water in the Opalinus Clay, Mont Terri, Switzerland, *Geochim. Cosmochim. Acta*, *66*(8), 1311–1321.
- Schmeling, E. E. (2014), Characterization of the hydrogeology and solute transport in a geologically complex, fractured, Late Cretaceous shale, Fort à la Corne kimberlite field, Saskatchewan, Canada, 162 pp., MSc thesis, Univ. of Saskatchewan.
- Sherwood Lollar, B., K. K. Hirschorn, M. M. G. Chartrand, and G. Lacrampe-Couloume (2007), An approach for assessing total instrumental uncertainty in compound-specific carbon isotope analysis: Implications for environmental remediation studies, *Anal. Chem.*, *79*(9), 3469–3475.
- Simpkins, W. W., and T. B. Parkins (1993), Hydrogeology and redox geochemistry of CH₄ in a Late Wisconsinian till and loess sequence in central Idaho, *Water Resour. Res.*, *29*(11), 3643–3657.
- Smith, L. A., S. L. Barbour, M. J. Hendry, K. Novakowski, and G. A. van der Kamp (2016), A multiscale approach to determine hydraulic conductivity in thick claystone aquitards using field, laboratory and numerical modeling, *Water Resour. Res.*, doi:10.1002/2015WR018448, in press.
- Szatkowski, B., S. Whittaker, and B. Johnston (2002), Identifying the sources of migrating gases in surface casing vents and soils using stable carbon isotopes, Golden Lake Pool, West-central Saskatchewan, In *Summary of Investigations 2002*, vol. 1, Saskatchewan Geological Survey, *Misc. Rep. 2002-4.1*, pp. 118–125, Sask. Ind. and Resour., Regina, Sask.
- Taylor, S. W., B. Sherwood Lollar, and L. I. Wassenaar (2000), Bacteriogenic ethane in near-surface aquifers: Implications for leaking hydrocarbon well bores, *Environ. Sci. Technol.*, *34*(22), 4727–4732.
- Tilley, B., and K. Muehlenbachs (2006), Gas maturity and alteration systematics across the Western Canada Sedimentary Basin from four mud gas isotope depth profiles, *Org. Geochem.*, *37*(12), 1857–1868.
- Tilley, B., and K. Muehlenbachs (2007), Isotopically determined Mannville group gas families, in *Let it Flow: Flow of Ideas, Hydrocarbons and Business, Proceedings of the 2007 CSPG CSEG Convention*. [Available at <http://cseg.ca/resources/abstracts>.]
- U.S. Energy Information Administration (2013), *Annual Energy Outlook 2013, with Projections to 2040*, U.S. Dep. of Energy, Washington, D. C.
- Van Loon, L. R., M. A. Glaus, and W. Müller (2007), Anion exclusion effects in compacted bentonites: Towards a better understanding of anion diffusion, *Appl. Geochem.*, *22*, 2536–2552.
- Vidic, R. D., S. L. Brantley, J. M. Vandenbossche, D. Yoxtheimer, J. D. Abad (2013), Impact of shale gas on regional water quality, *Science*, *340*(6132), 1235009-1–1235009-9, doi:10.1126/science.1235009.
- Waber, H. N., and J. A. T. Smellie (2008), Characterisation of pore water in crystalline rocks, *Appl. Geochem.*, *23*(7), 1834–1861.
- Wassenaar, L. I., and M. J. Hendry (1999), Improved piezometer construction and sampling techniques to determine pore water chemistry in aquitards, *Ground Water*, *35*, 1751–1760.
- White, D. J., G. Burrowes, T. Davis, Z. Hajnal, K. Hirsche, I. Hutcheon, E. Majer, B. Rostron, and S. Whittaker (2004), Greenhouse gas sequestration in abandoned oil reservoirs: The International Energy Agency Weyburn pilot project, *GSA Today*, *14*(7), 4–10, doi:10.1130/1052-5173(2004)014<4:GGSIAO>2.0.CO;2.
- Xia, X., and Y. Tang (2012), Isotope fractionation of methane during natural gas flow with coupled diffusion and adsorption/desorption, *Geochim. Cosmochim. Acta*, *77*, 489–503.
- Zhang, T., and B. M. Krooss (2001), Experimental investigation on the carbon isotope fractionation of methane during gas migration by diffusion through sedimentary rocks at elevated temperature and pressure, *Geochim. Cosmochim. Acta*, *65*(16), 2723–2742.